Mucoadhesive 3D printed vaginal ovules to treat endometriosis and fibrotic uterine diseases

Sarah Teworte , Simone Aleandri , Jessica Weber ,
Marianna Carone , Paola Luciani

PII: S0928-0987(23)00131-8
DOI: https://doi.org/10.1016/j.ejps.2023.106501
Reference: PHASCI 106501

To appear in: *European Journal of Pharmaceutical Sciences*

Received date: 23 March 2023
Revised date: 6 June 2023
Accepted date: 16 June 2023

Please cite this article as: Sarah Teworte , Simone Aleandri , Jessica Weber , Marianna Carone , Paola Luciani , Mucoadhesive 3D printed vaginal ovules to treat endometriosis and fibrotic uterine diseases, *European Journal of Pharmaceutical Sciences* (2023), doi: https://doi.org/10.1016/j.ejps.2023.106501

Highlights

- Vaginal drug delivery of pirfenidone, a repurposed candidate for endometriosis
- Semisoft 3D printed mucoadhesive ovule at a dose of 120 mg pirfenidone per ovule
- Pharmacopeial, *in vitro* release and *ex vivo* mucoadhesion assays for vaginal ovules
- 3D printed ovule showed sustained release and mucoadhesive properties
- 24 h exposure of endometriotic cells to pirfenidone required for therapeutic action

Mucoadhesive 3D printed vaginal ovules to treat endometriosis and fibrotic uterine diseases

Sarah Teworte, Simone Aleandri, Jessica Weber, Marianna Carone, Paola Luciani*

Department of Chemistry, Biochemistry and Pharmaceutical Sciences, University of Bern, Freiestrasse 3, 3012 Bern, Switzerland

*Emails to: paola.luciani@unibe.ch

Abstract

Gynaecological health is a neglected field of research that includes conditions such as endometriosis, uterine fibroids, infertility, viral and bacterial infections, and cancers. There is a clinical need to develop dosage forms for gynecological diseases that increase efficacy and reduce side effects and explore new materials with properties tailored to the vaginal mucosa and milieu. Here, we developed a 3D printed semisolid vaginal ovule containing pirfenidone, a repurposed drug candidate for endometriosis. Vaginal drug delivery allows direct targeting of the reproductive organs *via* the first uterine pass effect, but vaginal dosage forms can be challenging to self-administer and retain *in situ* for periods of more than 1–3 h. Here, we show that a semisoft alginate-based vaginal suppository manufactured using semisolid extrusion additive manufacturing is superior to vaginal ovules made using standard excipients. The 3D-printed ovule showed a controlled release profile of pirfenidone *in vitro* in standard and biorelevant release tests, as well as better mucoadhesive properties *ex vivo*. An exposure time of 24 h of pirfenidone to a monolayer culture of an endometriotic epithelial cell line, 12Z, is necessary to reduce the cells' metabolic activity, which demonstrates the need for a sustained release formulation of pirfenidone. 3D printing allowed us to formulate mucoadhesive polymers into a semisolid ovule with controlled release of pirfenidone. This work enables further preclinical and clinical studies into vaginally administered pirfenidone to assess its efficacy as a repurposed endometriosis treatment.

Key words: vaginal drug delivery, 3D printing, drug repurposing, fibrosis, endometriosis

Acronyms: API – active pharmaceutical ingredient; DoE – Design of Experiments; FDA – U.S. Food and Drug Administration; FDM – fused deposition modelling; GRAS – generally recognized as safe; IPF – idiopathic pulmonary fibrosis; SSE – semisolid extrusion; TGF-β – transforming growth factor β; USP, United States Pharmacopeia; VFS – vaginal fluid simulant.

Introduction

Leiomyoma (uterine fibroids) and endometriosis are gynaecological diseases that affect 70% of women [1] and 10% of reproductive-age women [2], respectively. Both diseases have fibrotic components: leiomyoma is characterized by fibrous tissue (fibroids) around the uterus [3] and endometriosis is characterized by fibrotic lesions on the peritoneum (in the case of superficial peritoneal endometriosis) and on the uterus, vagina, bladder, and bowel (in the case of deep infiltrating endometriosis) [4–8]. While the aetiology of neither disease is fully understood, fibrogenesis is thought to arise from somatic mutations of myometrial stem cells in leiomyoma [9] and from cyclic injury and repair in endometriosis [10]. Fibrosis has recently been proposed as a treatment target for both uterine fibroids [11] and endometriosis [10,12].

Pirfenidone is a small molecule drug which was approved for the treatment of idiopathic pulmonary fibrosis (IPF) by the European Medicines Agency in 2011 [13]. It is available as oral tablets containing 267 and 801 mg pirfenidone [14]. The daily dose of pirfenidone for IPF is 2403 mg [14], of which 70–80% is metabolized in the liver [13]. Pirfenidone modulates TGF-β [15], an inflammatory cytokine involved in fibrosis [16,17]. In leiomyoma, TGF-β not only stimulates cell proliferation and extracellular matrix deposition, but is also involved in excessive uterine bleeding [18]. In endometriosis, TGF-β stimulates collagen synthesis and endometrial stromal cell proliferation after implantation in the peritoneum [19]. Pirfenidone was shown to be effective at reducing fibrosis in preclinical models of leiomyoma [20] and abdominal adhesions [21]. In a prospective randomized double-blind clinical trial of 210 patients undergoing laparoscopic surgery for endometriosis, pirfenidone administered orally at a dose of 1800 mg/day for six months post-surgery was observed to reduce fibrotic adhesions compared to the control group that received placebo tablets [22]. However, side effects such as nausea, diarrhoea, rash and photosensitivity were reported frequently and the authors did not recommend pirfenidone because its adverse event profile outweighed its benefits [22].

Vaginal drug delivery has several therapeutic advantages compared to oral drug delivery. The large surface area and rich blood supply of the vagina [23,24] allow both hydrophobic and hydrophilic molecules to be absorbed [25], with high permeability for low molecular weight APIs [26]. The transit through the gastrointestinal tract and the resulting hepatic first pass effect can be avoided, requiring lower doses to be administered and thereby reducing adverse events [23,25–28]. Molecules absorbed in the upper third of the vagina are present at higher concentrations in and around the uterus than in systemic circulation, an effect known as the *first uterine pass effect* [29–34]. A locally elevated concentration of an API around the reproductive organs, achievable *via* vaginal administration, may improve the efficacy of the API and require a lower dose to be administered. Local delivery of hormonal

APIs for the treatment of endometriosis and uterine fibroids is reviewed in [35]. To our knowledge, nonhormonal APIs administered vaginally have thus far not been investigated for the treatment of leiomyoma nor endometriosis.

Different types of vaginal dosage forms exist, including pessaries/suppositories, ovules, rings, creams and gels. Vaginal dosage forms are typically employed for hormonal, antibacterial or antifungal therapies [25]. There are currently twelve marketed vaginal dosage forms for systemic and 34 for topical action [25]. Solid vaginal dosage forms allow precise dose control, easy administration, and are generally well accepted by patients [28,36,37], while vaginal creams and gels show better mucoadhesive properties, resulting in longer retention times on the vaginal wall [38]. Here, we develop a semisoft vaginal suppository that combines the advantages of solid and gel-like vaginal dosage forms, manufactured using 3D printing.

Additive manufacturing (3D printing) is an emerging field in drug delivery [39]. 3D printing not only allows personalized dosage forms to be manufactured but also for new materials to be used as excipients, resulting in improved drug product properties [39]. Two types of additive manufacturing are fused deposition modelling (FDM), which exploits the thermoplastic properties of a polymeric excipient; and semisolid extrusion (SSE), a type of 3D printing that relies on the rheological shear-thinning properties of a formulation to extrude it pneumatically [39]. While FDM has been used to manufacture personalized vaginal dosage forms such as vaginal rings [40], urogynaecological mesh implants [41,42], intrauterine devices [43], and vaginal suppository moulds [44], SSE is less well explored for applications in gynaecological drug delivery. One study used SSE to manufacture an endometrial stem cell-laden mesh as a potential treatment for pelvic organ prolapse [45]. The advantage of SSE over FDM is that it can be used to manufacture temperature-sensitive and gel-like formulations.

The lack of standardized *in vitro* tests hampers the development of effective vaginal dosage forms. The European Pharmacopeia's monograph on vaginal dosage forms merely states that a "suitable test" should be carried out to demonstrate the release of the API from dosage forms intended for prolonged local action [46]. Standard dissolution tests are not biorelevant for vaginal dosage forms because they are performed in volumes of 1–4 L. An ideal *in vitro* test would model the transport of the API through the vaginal wall into systemic circulation and several groups have developed *in vitro* tests for vaginal dosage forms [47–52]. There is also a lack of data on simulated vaginal fluids [53]: the majority of *in vitro* tests are performed using a vaginal fluid simulant developed by Owen & Katz based on a review of studies published between 1925 and 1997 [54]. A more recent study by Rastogi *et al.* gives a simulated cervicovaginal fluid recipe based on 13 samples [55]. Here, we employ an *in vitro*

test adapted from Tietz & Klein [52] to estimate the rate of pirfenidone transport through the vaginal mucosa into systemic circulation.

In this work, we develop vaginal suppositories containing pirfenidone for local delivery to the reproductive organs using excipients generally recognised as safe by the U.S. Food and Drug Administration (FDA). We develop a semisolid vaginal suppository containing pirfenidone and, for comparison, manufacture pirfenidone-containing ovules according to standard pharmaceutical recipes based on Macrogol, a hydrophilic excipient, and Witepsol, a hard fat. The suppositories and ovules were analysed *in vitro* to estimate the transport of pirfenidone from the vaginal mucosa into systemic circulation; *ex vivo* for their mucoadhesion; and pirfenidone *in vitro* on an immortalized human endometriotic cell line. In doing so, we not only develop the first vaginal dosage form for pirfenidone, but also demonstrate the advantages of SSE for manufacturing vaginal dosage forms.

2. Materials and methods

2.1 Chemicals

Pirfenidone (5-methyl-1-phenylpyridin-2(1H)-one) was purchased from BLD Pharm, Germany. Agarose, sodium alginate (product number W201502, quality level 400, viscosity of 5.0–40.0 cps in a 1% solution in water at 25 °C), and hydroxypropylmethylcellulose (HPMC, product number 423203, molecular mass ~86,000, viscosity of 2663–4970 cps in a 2% solution in water) were purchased from Sigma Aldrich, USA. Sodium acetate, acetic acid, trifluoroacetic acid (TFA), calcium chloride, HEPES, and phosphate buffered saline (PBS) were purchased from Carl Roth, Germany. Witepsol® S 58 was kindly gifted by IOI Oleo, Germany. Caffeine, glucose monohydrate, lactic acid, Macrogol 400, and Macrogol 1500 were purchased from Hänseler, Switzerland. Acetonitrile was purchased from Thermo Fisher Scientific, USA. Sodium lactate solution 50% was purchased from VWR, USA. Ultrapure water with a resistivity of 18.2 MΩ·cm was produced by a Barnstead Smart2pure device (Thermo Fisher Scientific).

2.2 Production of standard vaginal ovules

Macrogol and Witepsol ovules were manufactured according to the Münzel method, a conventional method used in pharmaceutical production of vaginal ovules, shown schematically in **Fig. 1(a)**. For Macrogol ovules, the base composition was Macrogol 1500 (92 m/m%), Macrogol 400 (4 m/m%) and lactic acid (2 m/m%). For Witepsol ovules, the base composition was 100% Witepsol® S 58. Half of the base was mixed with pirfenidone, melted

at 70 °C in a water bath, and poured into an ovule mould. The other half of the base was melted and poured onto the hardened half-ovules. The solidified ovules were removed from the mould, melted down, re-poured into the mould and left to solidify at 4 °C for 30 min.

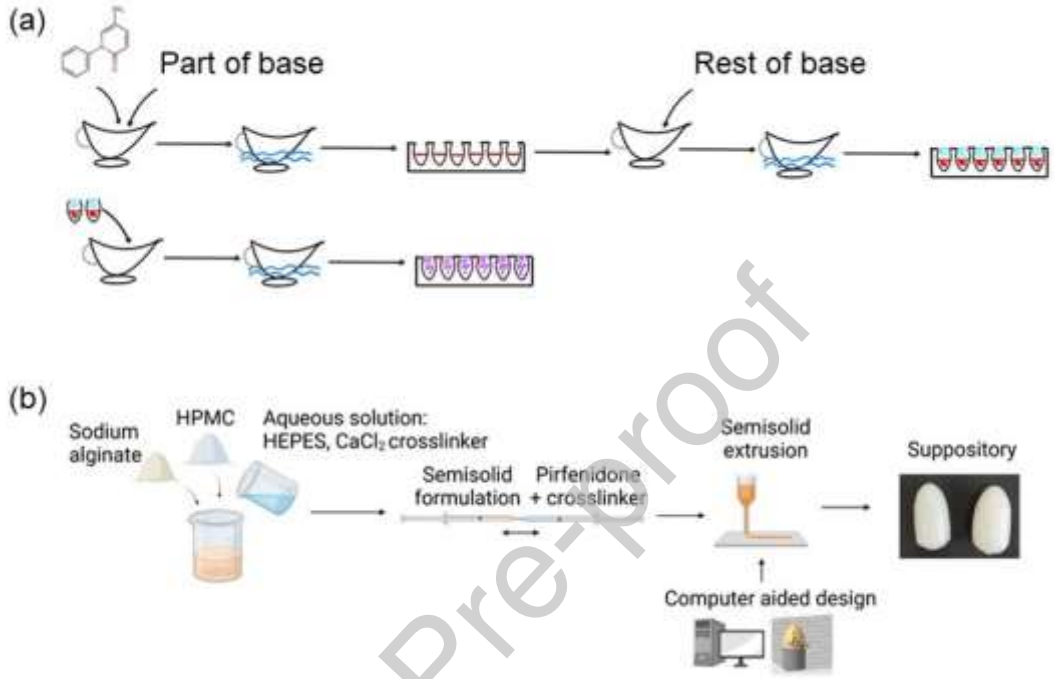

Figure 1. Schematic representations of (**a**) the Münzel method for ovule production used to produce Macrogol and Witepsol ovules; (**b**) the production of 3D printed ovules. Figure 1 (**b**) was created using BioRender.com.

2.3 3D printed ovules

2.3.1 Formulation screening to find a formulation suitable for semisolid extrusion

Sodium alginate and HPMC were chosen due to their mucoadhesive properties and because they are generally recognised as safe (GRAS) by the FDA. To find a 3D-printable alginate/HPMC formulation, a Design of Experiments approach was used. A mixture extreme vertices design was employed with lower and upper bound constraints on the alginate, HPMC and buffer (HEPES 30 mM, $CaCl_2$ 15 mM) content. The lower/upper bounds on the mixture extreme vertices design were 2.0/10.0 m/m% for alginate and HPMC, and 80.0/90.0 m/m% for buffer, respectively. The composition of 11 formulations within these bounds was determined using a statistical software programme (Minitab® 18.1, USA). The composition of each formulation is provided in the Supplementary Information (**Fig. S1**, **Table S1**).

Three dependent variables were measured for each formulation: the mean storage modulus G', viscosity at rest, and printability, assessed as a score on a scale of 1 (worst) to 6 (best) based on the definition of the extruded shape. Statistical analysis methods are described in Section 2.10.

2.3.2 Rheology

The rheological properties of each formulation were investigated using a Modular Compact Rheometer MCR 72 (Anton Paar, Graz, Austria) equipped with a cone-plate geometry, diameter 49.942 mm and cone angle=0.993°. The temperature was kept at 25 °C and the linear viscoelastic region (LVR) was determined by conducting an amplitude sweep at 1 Hz between 0.01 and 100% strain.

2.3.3 Printability screening

Each formulation was extruded through a 22G nozzle at pressure 20–200 kPa, speed 5 mm/s and the extruded shape given a score on a scale of 1 (worst) to 6 (best) based on the definition of the extruded shape.

2.3.4 Production method

3D printed ovules were produced using semisolid extrusion additive manufacturing, as shown in **Fig. 1(b)**. Sodium alginate (10 m/m%) and HPMC (10 m/m%) were mixed with an aqueous solution containing HEPES (30 mM) and calcium chloride (15 mM) (80 m/m% buffer), heated to 80 °C for 15 min and stirred overnight. The semisolid bulk was transferred into a syringe and centrifuged at 4430 *g* for 15 min. To add pirfenidone, a dual syringe method was used: a syringe containing 2.25 mL semisolid formulation was connected to another syringe containing 0.75 mL pirfenidone and calcium chloride (20 mM) in acetate buffer (50 mM, pH 5.2) using a Luer lock. This volume was sufficient to manufacture one suppository. The syringes were pushed back and forth fifty times to create a homogeneous formulation. The formulation was transferred into the 3D printing cartridge and centrifuged at 4430 *g* for 15 min to remove air bubbles. The vaginal suppository was designed using the Netfabb® computer-aided design software (Autodesk, USA). The formulation was pneumatically extruded into the designed shape using a BIO X 3D printer (Cellink, Sweden). The following printing parameters were used: pressure 80 kPa; print speed 5 mm/s; layer height 0.20 mm; infill density 30%; infill pattern honeycomb; nozzle diameter 22G. For post-

print crosslinking, ovules were placed in 5 mL of crosslinking buffer ($CaCl_2$ 100 mM in ultrapure water) for 20 min. For experiments, ovules were removed from the crosslinking buffer, residual surface water removed by blotting with a lint-free tissue, and ovules used for experiments immediately.

2.4 Pharmacopeial tests

The European Pharmacopeia prescribes several quality tests for solid vaginal dosage forms. Uniformity of mass and content describe the intra-batch variability in mass and API content of the dosage forms, respectively. The dissolution test is used to measure the time taken for the dosage form to dissolve or soften in 4 L of dissolution medium.

2.4.1 Uniformity of mass, content

Uniformity of mass was tested according to Ph. Eur. 2.9.5 on a batch of 10 ovules. Uniformity of content was tested according to Ph. Eur. 2.9.6 (Test B) on a batch of 10 ovules. Ovules were dissolved in ultrapure water, an aliquot lyophilized, the lyophilizate dissolved in the mobile phase, and the pirfenidone content quantified using the HPLC-DAD method described below.

2.4.2 Disintegration tests

The disintegration behaviour of ovules was tested according to Ph. Eur. 2.9.2 using an ERWEKA ST 35 rotating basket apparatus with a volume of 4 L. The medium was 10 mM acetate buffer at pH 4.2 and temperature 37 °C. The dosage form was placed in the basket and the time to disintegration measured. For ovules that did not dissolve rapidly, the consistency after 1 h was assessed manually. As described in the Ph. Eur., a dosage form that had softened passed the test, but a dosage form that did not soften nor dissolve failed [56].

2.5 Shake flask test

A volume of 20 mL of vaginal fluid simulant (VFS) [55] was filled into shake flasks with lids and left to equilibrate in a shaking incubator at 37 °C. One ovule was added to each shake flasks and 5 mL aliquots taken every hour for 8 h. At each time point, aliquoted medium was replaced immediately with temperature equilibrated VFS. Experiments were performed under sink conditions (medium able to dissolve at least 3· the amount of API in the dosage form). Samples were lyophilized for HPLC-DAD analysis, described below.

2.6 Bespoke release test

A bespoke release test modelling the transport of API from the vaginal mucosa into systemic circulation was adapted from [52]. The apparatus consisted of an inner and an outer chamber separated by an agarose wall, shown schematically in **Fig. 2**.

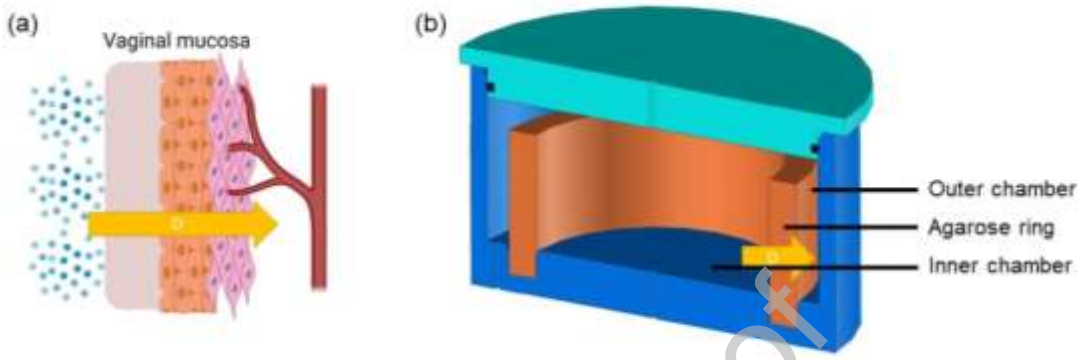

Figure 2. (a) Schematic representation of the diffusion path (yellow arrow) of a small molecule API across the vaginal mucosa into systemic circulation; (b) diagram of the bespoke release apparatus adapted from [52] showing the analogous diffusion path (yellow arrow).

The method described in [52] was followed. Containers were manufactured from polylactic acid using fused deposition modelling. Agarose rings (2 m/m% in ultrapure water) were made by moulding and inserted into the PLA containers. The inner chamber was filled with 13 mL VFS [55] and the outer chamber with 8.5 mL PBS. The system was pre-equilibrated at 37 °C in a shaker incubator. The vaginal dosage form was placed in the inner chamber. Samples were taken from the inner and outer chambers every hour for 8 h and at 24 h with immediate replacement of medium. Experiments were performed under sink conditions (medium able to dissolve at least 3· the amount of API in the dosage form). Samples were lyophilized for HPLC-DAD analysis, described below. At the end of the release test, pirfenidone was extracted from the agarose ring by successive cycles of freezing (-80 °C, 16 h) and thawing (37 °C, 32 h) until no more pirfenidone was present. As described by Tietz, the pirfenidone release profile corresponds to the sum of pirfenidone released into the inner and outer chambers.

2.7 HPLC-DAD

Pirfenidone was quantified using an HPLC-DAD method developed in our laboratories. Briefly, an Ultimate 3000 HPLC system (Thermo Fisher Scientific, Reinach, Switzerland) with

a NUCLEOSIL 100-5 C18 column (particle size 5.0 µm, length 250 mm, internal diameter 4.0 mm) (Macherey-Nagel, Düren, Germany) was used. The mobile phase composition was 65 v/v% acetonitrile +0.1 v/v% trifluoroacetic acid, 35 v/v% ultrapure water +0.1 v/v% trifluoroacetic acid, the flow rate 0.7 mL/min, the injection volume 5 µL and the temperature 25 °C. Pirfenidone was detected at λ = 317 nm and the internal standard, caffeine (20 µg/mL), at λ = 278 nm.

2.8 Mucoadhesion assay (*ex vivo*)

Porcine vagina ≤6 after slaughter (Metzgerei Wütrich, Münchenbuchsee, Bern, Switzerland) was used to assess the properties of 3D printed ovules *ex vivo* according to the protocol described in [57] and reviewed in [58]. Briefly, the reproductive organs were separated from proximal organs (urethra, bladder, intestine) using a scalpel. The vagina was cut into 5 cm pieces. Each vagina piece was closed with a clip at one end, the ovule inserted, and the vagina clipped closed at the other end. Each piece was placed in 70 mL pre-equilibrated acetate buffer (30 mM, pH 4.2) and incubated in a shaker incubator at 37 °C for 3 or 16 h. The vagina pieces were sliced open longitudinally to visualize the ovule's dissolution on the vaginal mucosa.

2.9 Cell culture

Immortalized human epithelial endometriotic cells (12Z cell line [59]) were purchased from Applied Biological Materials, Canada. 12Z cells were cultured at 37 °C in a humidified atmosphere containing 5% CO_2. The complete growth medium composition was Dulbecco's Modified Eagle Medium (DMEM) with 4.5 g/L glucose, without sodium pyruvate (Carl Roth, Karlsruhe, Germany, Ref 9091.1), 10 v/v% fetal bovine serum (Merck KGaA, Darmstadt, Germany, Ref ES-009-B), 200 mM L-glutamine (gibco, Life Technologies Limited, Paisley, UK, Ref 25030-024) and 1 v/v% penicillin-streptomycin (gibco, Life Technologies Corporation, Grand Island, NY, USA, Ref 15140-122). Subcultivation was performed with 0.05% Trypsin-EDTA. Cells were seeded in 75 cm^2 tissue culture flasks (TPP) at a density of $0.1 \cdot 10^6$ cells per flask and harvested at 80–90% confluency.

For experiments, cells with passage number 10 were used. Cells were seeded on transparent 96 well plates (TPP) at a density of 15,000 cells per well in complete growth medium and incubated for 24 h prior to treatment with serum-free medium (DMEM, 4.5 g/L glucose, without sodium pyruvate, 200 mM L-glutamine, 1 v/v% penicillin-streptomycin). Cells were treated with pirfenidone at concentrations in the range 0.25–1.25 mg/mL for 2, 6

and 24 h. Cytotoxicity was evaluated using a CCK-8 cell proliferation assay as described in [60]. Briefly, 90 µL serum-free DMEM supplemented with 1 v/v% penicillin/streptomycin and 10 µL CCK-8 were added to each well. 12Z cells were incubated for 2 h at 37 °C, 5% CO_2. The absorbance was measured at 450 nm using a plate reader (Spark 10M, Tecan, Switzerland). To calculate the cell metabolic activity in percent, the following equation was used. *Cell metabolic activity (%) = (OD sample/OD control) × 100* where "OD sample" refers to the optical density of the cells treated with pirfenidone and "OD control" is the cells exposed to DMEM supplemented with 1 v/v% penicillin/streptomycin only.

2.10 Statistical analysis

All results are reported as mean ± standard deviation of three independent replicates. Statistical analysis was performed using Minitab and Prism 9 (GraphPad, USA).

For analysis of the formulation screening, data was fitted by a cubic equation for three components in Minitab. To determine whether the association between the response and each term in the model was statistically significant, the *p*-value of each term was compared to the significance level to assess the null hypothesis. If the *p*-value of a term was greater than the significance level (p>0.05), the model was reduced by eliminating statistically insignificant terms using stepwise regression. By using this tool, the software systematically added the most significant variable or removed the least significant variable during each step. *S (the average distance between the observed values and the regression line)*, R^2, *R^2 adjusted* and *R^2-predicted* (provided in the Supplementary Information) were used to determine how well the model fitted the data. The response optimization was used to identify the best formulation composition.

3 Results

3.1 3D printed ovules formulation development

Rheology studies provide information on the viscosity and elasticity of a material and enable the properties of the fluid to be correlated to its printability *via* a Design of Experiments approach. Design of Experiments not only allowed us to find an optimal formulation for 3D printing, but also to evaluate how each parameter of the formulation affected the printability and viscosity. Instead of using a trial-and-error approach, in which a large number of combinations is tried to identify an ideal formulation and then test the formulation's quality (*Quality by Testing*), Design of Experiments allows an entire design space to be evaluated

using a minimum number of experiments. When a range of each independent variable is defined, Design of Experiments determines statistically which values of each independent variable to measure experimentally and then allows the response of each dependent variable to be modelled in the entire design space. Design of Experiments not only reduces the number of experiments while maximizing the output; it also gives insights into the decision-making process of optimization, as highlighted by the FDA (FDA 2007; ICH Q8 guidelines).

Based on the response of the three dependent variables, the statistical software fitted the model with a special cubic equation and evaluated the *p* value of each term in the equation against a significance threshold. If the *p* value of a term in the cubic equation was greater than 0.05, the term was removed and the process repeated using stepwise regression. The *S*, R^2, R^2 *adjusted* and R^2 *predicted* values were used to determine how well the model fitted the data. **Table S1** (supplementary material) shows the estimated regression coefficients and model summary for the printability score (Tables S2 and S3, respectively), viscosity (Tables S4 and S5, respectively), and storage modulus (Tables S6 and S7, respectively). Data on printability score and viscosity fitted the model well, while for the storage modulus, *G'*, the model fitted the data poorly. Therefore, *G'* was eliminated and the Design of Experiments analyzed for a double response with equal importance given to printability score and viscosity. **Fig. 3** shows the rheological and printability screening of the alginate/HPMC formulations. The best printable formulations were in the middle of the design space [**Fig. 3(a)**] and formulations with a low buffer content and approximately equal alginate and HPMC content had favourable viscosity properties for semisolid extrusion [**Fig. 3(b)**]. In the linear viscoelastic region, the storage modulus is greater than the loss modulus, indicating a gel-like structure [**Fig. 3(d)**]. The formulation has shear-thinning behaviour, making it suitable for semisolid extrusion 3D printing [**Fig. 3(e)**].

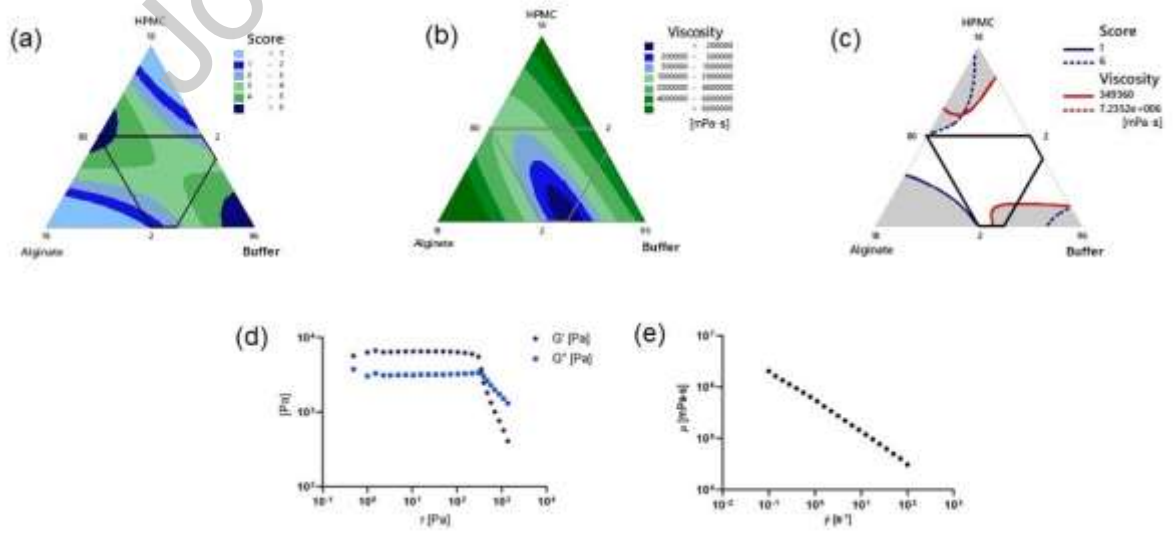

Figure 3. Response surface of (**a**) printability score and (**b**) viscosity at rest, (**c**) composite contour plot showing how the composite response (printability score, viscosity) rates to the proportion of each component in the formulation (alginate, hydroxypropylmethylcellulose (HPMC), buffer). (**d**) Amplitude sweep and (**e**) viscosity curve of the best-performing formulation. *G'* storage modulus, *G"* loss modulus, τ shear stress, shear strain, $\dot{\gamma}$ shear rate

Figure 3(c) shows the composite contour plot, summarizing how the component response (printability score, viscosity) relates to the proportion of each component in the formulation. An overlaid contour plot allows us to visually identify an area of the design space in which a formulation performs well in all response variables. Each set of contours defines the boundaries of acceptable values of the fitted response. All points that have the same low response are linked to produce contour solid lines of constant responses while all points that have the same high response are linked to produce contour dashed lines of constant response. The white contour area in the plot displays the combination of values for that yield satisfactory fitted values for the printability score and viscosity, given the holding values for the other three variables. Therefore, any variable settings that fall in the white region produce a product with acceptable mean responses.

The software tool allowed us to evaluate the impact of alginate, HPMC and buffer content on the printability and viscosity. The response optimization was used to identify the component proportions that simultaneously yielded the most desirable printability score and viscosity, expressed as a composite desirability. To create the optimization plot, the default value of 1 for the desirability of each dependent variable was used. The optimal solution occurred where the composite desirability was maximised. The best formulation had a composition of 10 m/m% alginate, 10 m/m% HPMC and 80 m/m% buffer.

3.2 Visual appearance and quality of ovules

Vaginal ovules, also known as pessaries or suppositories, are typically manufactured by moulding. The excipients and API are gently heated and poured into moulds to solidify. Classical ovules obtained with two different bases, Macrogol and Witepsol, are shown in **Fig. 4(a)** and **Fig. 4(b)**, respectively. 3D printed ovules are shown in **Fig. 4(c)**. All ovules had a homogeneous visual appearance and were rigid and easy to handle manually. Visual appearance is an important quality attribute for pharmaceutical dosage forms, with one study indicating that patients prefer white as a colour for vaginal dosage forms [61], suggesting all three types of ovule would be acceptable to patients.

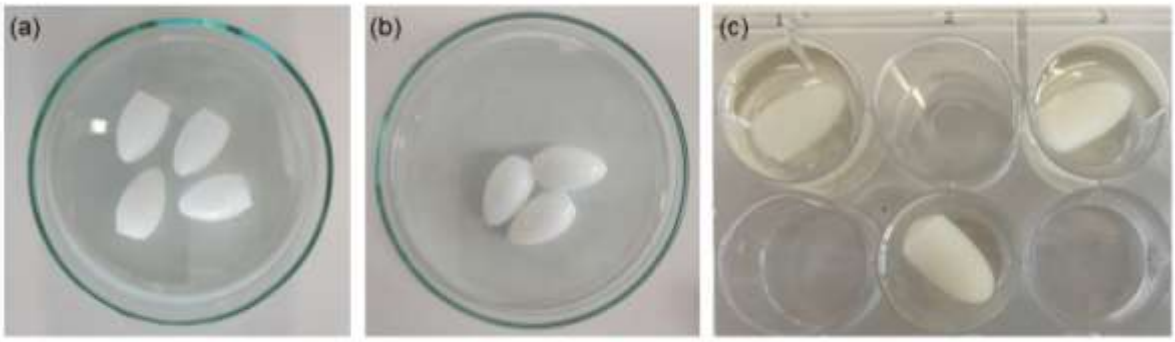

Figure 4. (**a**) Macrogol, (**b**) Witepsol, and (**c**) 3D printed ovules.

To manufacture the 3D printed dosage forms, alginate and HPMC were mixed with buffer, pirfenidone and an ionic crosslinker added using the dual syringe method, the formulation transferred into the semisolid extrusion cartridge and printed at a pressure of 80 kPa. Printlets were ionically crosslinked by immersing the printed ovules in 5 mL crosslinking buffer for 20 min post-print. 87.1 ±0.4% of pirfenidone remained in the ovule and 12.9 ±0.4% of pirfenidone leaked into the crosslinking buffer. Results of pharmacopeial quality tests performed on Macrogol, Witepsol and 3D printed ovules are summarized in **Table 2**. Macrogol, Witepsol and 3D printed ovules passed Uniformity of Mass and Content tests. Macrogol and Witepsol ovules dissolved rapidly in the dissolution test, while 3D printed ovules softened after 1 h in the dissolution medium. 3D printed ovules were rigid and easy to handle manually.

Table 2. Pharmacopeial tests performed on Macrogol, Witepsol and 3D printed ovules

Ovule	Uniformity of mass (Ph. Eur. 2.9.5)	Uniformity of content (Ph. Eur. 2.9.6)	Disintegration (Ph. Eur. 2.9.2)
Macrogol	Mean mass: 3.01 ±0.03 g None >2% from mean	Mean content: 128 ±5 mg None >6% from mean	Disintegrated within 15 min
Witepsol® S 58	Mean mass: 2.51 ±0.01 g None >1% from mean	Mean content: 118 ±7 mg None >13% from mean	Disintegrated within 15 min
3D printed	Mean mass: 2.13 ±0.10 g 8 ovules within 5%, two within 10% of mean	Mean content: 122 ±14 mg All but one ovule <15% from mean, one ovule 17% from mean	Softened after 1 h

3.3 In vitro release tests

The release of pirfenidone from the ovules was followed for 8 h using a standard shake flask method and an agarose ring setup developed by [52]. The agarose ring setup provides a more biorelevant assay, as the agarose ring presents a diffusion barrier analogous to the vaginal mucosa [52].

Pirfenidone was rapidly liberated from Macrogol and Witepsol ovules, with 92–100% released after 3 h. In a shake flask setup, 3D printed ovules released pirfenidone more slowly, with 82–90% released after 8 h **[Fig. 5(a)]**. In the release profiles from a bespoke apparatus containing an agarose ring as a diffusion barrier, Macrogol and Witepsol ovules showed similar release behaviour to a solution of free pirfenidone [**Fig. 5(b)**]. Pirfenidone was released more slowly from 3D printed ovules in the agarose ring assay, with 70–75% of pirfenidone released from 3D printed ovules after 8 h [**Fig. 5(b)**]. The release of pirfenidone into the inner and outer chambers separately is shown in Supplementary Figures S2, S3 and S4 for Macrogol, Witepsol and 3D printed ovules, respectively.

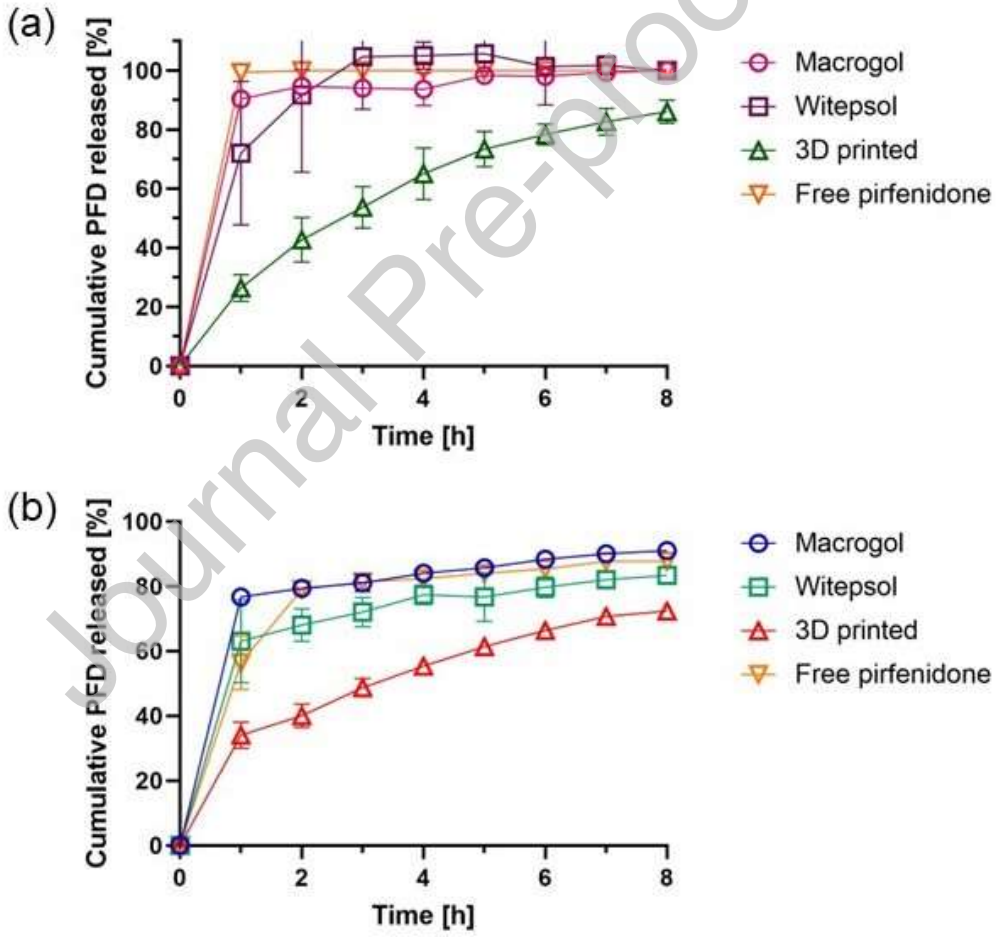

Figure 5. *In vitro* release of pirfenidone from Macrogol, Witepsol and 3D printed ovules in vaginal fluid simulant [55] in (**a**) a shake flask and (**b**) a bespoke release test adapted from [52]. Results are shown as mean ±SD (n = 3).

3.4 Ex vivo mucoadhesion

The softening of the 3D printed ovule into a mucoadhesive hydrogel on *ex vivo* porcine vaginal tissue was assessed qualitatively [**Fig. 6]**. Porcine vaginal tissue was gathered at slaughter and stored for <6 h at 4 °C. The vagina was cut into 5 cm pieces, the ovule inserted without rinsing the mucosa, and the tissue closed at either end to create a sack which was suspended in acetate buffer at pH 4.2. After 3 or 16 h, the tissue was removed from the buffer and the vagina cut open longitudinally to visualize the ovule. Ovules with Macrogol and Witepsol excipients dissolved completely within 3 h [**Fig. 6(a), (b)**]. 3D printed ovules disintegrated partially in 3 h [**Fig. 6(c)**] and fully after 16 h, forming a mucoadhesive hydrogel [**Fig. 6(d)**]. Our observations suggest that the hydrogel formed by the ovule may allow a longer retention time *in vivo* compared to standard fast-dissolving excipients such as Macrogol and Witepsol.

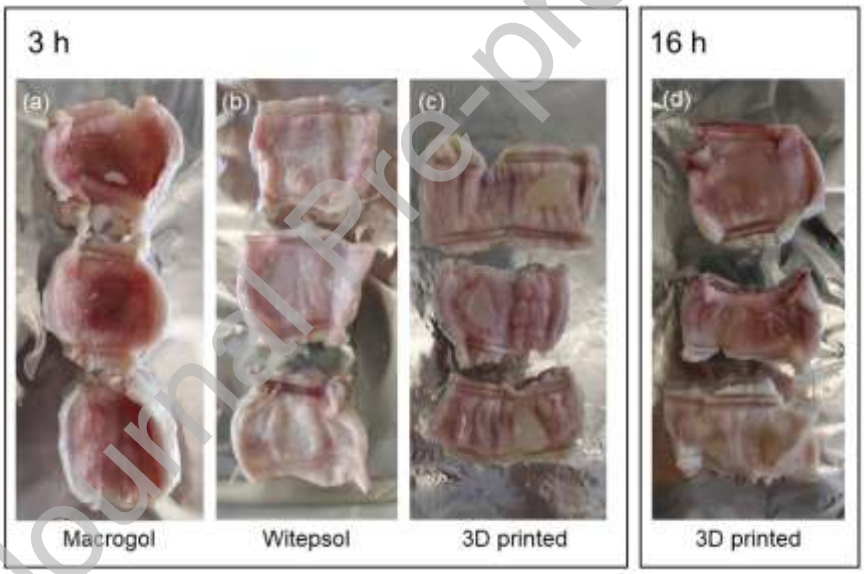

Figure 6. Representative images of (**a**) Macrogol, (**b**) Witepsol, (**c**) 3D printed ovules incubated in *ex vivo* porcine vagina for 3 h, and (**d**) 3D printed ovules incubated in *ex vivo* porcine vagina for 16 h

3.5 Effect of pirfenidone on metabolic activity of 12Z cells

The effect of pirfenidone on the metabolic activity of an epithelial cell line derived from endometriotic lesions, 12Z [59], was studied to estimate the target concentration of pirfenidone and exposure time of endometriotic lesions to pirfenidone. We chose 12Z cells as an ideal *in vitro* model recapitulating many properties of endometriotic lesions, such as

epithelial-to-mesenchymal transition, invasion and migration [62,63]. The influence of different pirfenidone concentrations and incubation times on the 12Z cells' metabolic activity was quantified with a CCK-8 assay, a colorimetric method based on the reduction of tetrazolium salt by cellular dehydrogenases.

Pirfenidone concentrations up to 1.25 mg/mL did not affect the metabolic activity of 12Z cells when cells were exposed to pirfenidone for 2 h and 6 h [**Fig. 7**]. At 24 h exposure time, high pirfenidone concentrations tended to reduce the metabolic activity of 12Z cells [**Fig. 7**]. This indicates that sustained (24 h) high concentrations of pirfenidone (>1 mg/mL) in and around endometriotic lesions are required for pirfenidone to be efficacious at reducing the metabolic activity of endometriotic epithelial cells. To achieve this, a dosage form that releases sufficiently high amounts of pirfenidone for long time periods is required.

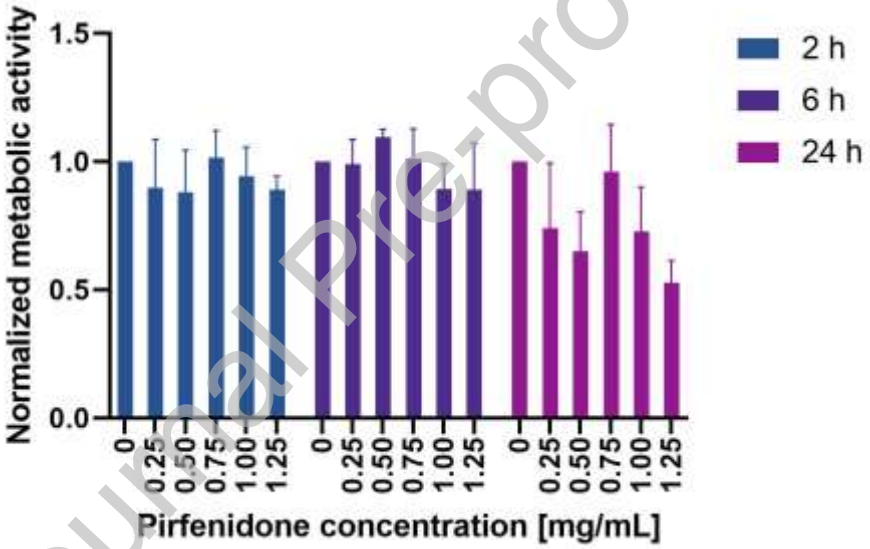

Figure 7. Metabolic activity of 12Z cells (normalized to starved) against pirfenidone concentration at incubation times of 2, 6, and 24 h. Results are shown as mean ±SD (n = 3).

4. Discussion

Endometriosis is a chronic gynaecological disease for which medical treatments need to be developed. Recently, the fibrotic aspect of the disease has emerged as a potential therapeutic target [5,10,19,64]. Pirfenidone is an antifibrotic drug marketed as an oral tablet, which in a clinical trial was shown to be efficacious for endometriosis but not recommended due to its adverse event profile [22]. Here, we propose vaginal administration of pirfenidone for endometriosis treatment and develop vaginal dosage forms containing pirfenidone.

Various vaginal dosage forms containing steroids have been developed and are used for endometriosis treatment [35]. To our knowledge, this is the first time an API targeting nonhormonal pathways has been formulated for vaginal drug delivery for endometriosis.

Vaginal drug delivery has the advantage of avoiding the hepatic first pass effect, reducing the dose and the administration frequency, and potentially increasing therapeutic efficacy [65]. Different types of vaginal dosage forms each have their respective advantages: gels are comfortable to insert and can be formulated with mucoadhesive polymers, while solids allow precise dosage and easy insertion [61]. Semisolid dosage forms are generally preferred by patients [61,66]. Vaginal rings have the advantage of sustained release over a period of up to a year [61], but vaginal rings may be painful for patients with dyspareunia (pain upon vaginal penetration, reported by 50% endometriosis patients [67]) due to the ring's size and rigidity. There is a need for a new vaginal formulation that combines the advantages of solid and gel-like dosage forms, for which semisolid ovules and vaginal films have been proposed.

Recently, vaginal films have been developed preclinically for antifungal, antiviral and nonhormonal contraceptive purposes [61,68,69], and some films are being explored in Phase I clinical trials [70,71]. In studies comparing films to semisoft suppositories, participants expressed broadly equal preference for both [61]. A limitation of vaginal films is that patients frequently report difficulty inserting the film [61], making it challenging to insert the dosage form into the upper third of the vagina, where the first uterine pass effect acts [29,34]. We chose to design a semisolid ovule because ovules are easier to handle manually, to insert high into the vagina, and are a common dosage form, potentially enabling more rapid clinical translation.

Standard vaginal ovules contain hydrophilic excipients, such as Macrogols, or lipophilic excipients, such as hard fats. They dissolve quickly, but have the disadvantage of poor retention and mucoadhesion. Here, excipients for standard ovules were chosen based on a literature review [72] and a review of compendium.ch, a database of medicines approved in Switzerland. We chose to manufacture Macrogol and Witepsol ovules as standard dosage forms.

As a third formulation, we developed an alginate/HPMC mucoadhesive polymer mixture and screened for the best composition for semisolid extrusion. The formulation cannot be manufactured using moulding because moulding does not allow the ovule to be crosslinked efficiently from a gel-like into a solid dosage form. Semisolid extrusion additive manufacturing not only allows the ovules to be ionically crosslinked post-print so they become solid and easy to handle manually; but 3D printing also allows the size and shape of ovules to be adapted easily, enabling an ovule's volume and dose to be adjusted to suit an individual patient or a subgroup of patients [39].

Macrogol, Witepsol and 3D printed ovules were compliant with all pharmacopeial quality tests for vaginal dosage forms. In the dissolution test, 3D printed ovules did not fully dissolve, but softened, meeting pharmacopeial dissolution test requirements [56].

The daily oral dose of pirfenidone for idiopathic pulmonary fibrosis, pirfenidone's approved indication, lies at 600 mg/day in the first 14 days, and 1800–2400 mg/day thereafter [13]. Of the oral dose, 70–80% is lost during first pass metabolism in the liver, leaving 20–30% of the oral dose bioavailable [13]. This corresponds to 120–180 mg pirfenidone per day in the low dose regimen, and 360–730 mg/day in the high dose regimen. Since vaginal ovules deliver the drug locally to the reproductive organs, we estimate an effective therapeutic dose to be at the low end of this range, i.e., 120 mg/day.

With the appropriate design of a dosage form, it is possible to control the release rate of a drug and in turn the efficacy and safety of a treatment, as it allows drug plasma concentrations to be within the therapeutic window for an extended time period [73]. To qualitatively infer an expected pharmacokinetic profile, it is pivotal to determine the release profile of a drug *in vitro* using a biorelevant setup.

The shake flask release test, with its simple setup to screen the rate of release of an API, is a commonly employed method, especially when carried out using simulated vaginal fluid [74]. In our setup, Macrogol and Witepsol ovules were shown to rapidly liberate pirfenidone, which may be undesirable, as it may result in an unfavourable pharmacokinetic profile. 3D-printed ovules released pirfenidone more slowly in the shake flask. Despite its convenience and its widespread use, a shake flask method is not representative of the complex vaginal physiology: the 20 mL release volume is not biorelevant and it does not enable to establish whether pirfenidone is absorbed through the vaginal mucosa and, in turn, into systemic circulation.

There are several proposed bespoke release test setups which mimic vaginal conditions more closely and are thus more biorelevant [51]. A small volume apparatus of type 4 in the US Pharmacopeia (USP) [75] allows dissolution in a smaller volume to be tested, however, it only gives the release of pirfenidone in vaginal fluid. Similar apparati with smaller volumes have been proposed in [48,49] and have limitations regarding their biorelevance. Another design that uses *ex vivo* tissue [47] may enable the mucoadhesion of a dosage form to be quantified, but this apparatus did not use a biorelevant medium nor was the flow rate controlled [51]. A lack of a standardized, well-evidenced cervicovaginal simulant fluid further hinders the development of meaningful *in vitro* tests for vaginal dosage forms. Changes in composition and properties of in cervicovaginal fluid during the menstrual cycle may affect the rate of ovule dissolution and drug release. More data from human samples is required to fully characterize these fluctuations and to be able to recapitulate them *in vitro*.

An apparatus developed by Tietz & Klein uses an agarose boundary to model the vaginal mucosa [52]. Agarose has been proposed as a material suitable for mimicking living tissue for *in vitro* drug diffusion studies, and agarose gel set-ups are considered more realistic than bulk fluid setups [76]. In a dissolution study of free pirfenidone, the agarose ring setup limited the drug's diffusion compared to the shake flask assay. Adapting the bespoke release test from [52], we could estimate how much pirfenidone is transported through the vaginal mucosa and into systemic circulation. The device was qualified by Tietz & Klein with an *in vitro–in vivo* correlation for two molecules, etonogestrel (324 g/mol, logP 3.3) and ethinyl estradiol (296 g/mol, logP 3.7) [52]. Compared to these two molecules, pirfenidone is smaller (185 g/mol) and more hydrophilic (logP 2.1). We expect pirfenidone to diffuse through the agarose boundary more quickly than etonogestrel and ethinyl estradiol due to its smaller size and more hydrophilic properties. On the one hand, the rate of diffusion of pirfenidone through the agarose boundary may be slower due to its smaller size; on the other hand, its more hydrophilic properties allow it to diffuse more quickly than etonogestrel and ethinyl oestradiol. While a lack of *in vivo* data for vaginally administered pirfenidone prevents us from knowing whether this bespoke apparatus gives an accurate transport rate of pirfenidone through human vaginal mucosa, the test gives a better estimate compared to a simple shake flask setup and allows us to compare dosage forms before proceeding to *in vivo* studies. In the bespoke release test, Macrogol and Witepsol ovules released pirfenidone at a rate similar to a free pirfenidone solution, while 3D printed ovules released pirfenidone more slowly, facilitating a better-controlled pharmacokinetic profile which we expect to see mirrored in *in vivo* studies.

To better understand the dissolution behaviour of ovules on vaginal mucosa, *ex vivo* experiments on porcine vagina were performed. Porcine vagina has been used previously for *ex vivo* tests of vaginal dosage forms in academic research and commercial product development [53,77–79]. *Ex vivo* porcine vagina has been shown to have good similarity with human *ex vivo* vaginal tissue in terms of histology and permeability to molecules including tritiated water and vasopressin [79,80]. Major differences of porcine vagina compared to human are that porcine vagina has a pH of 7 rather than 4; its rugae run longitudinally rather than transverse; it experiences an oestrous rather than a menstrual cycle; and its microbiota differs. For the permeation of 17β-oestradiol, r-arecoline, and oxytocin, statistically significant differences were found between porcine and human *ex vivo* vaginal mucosa [80]. Nevertheless, the behaviour of ovules on *ex vivo* porcine vaginal mucosa provides qualitative information on the ovules' dissolution that is no less valuable than studies on bovine or ovine *ex vivo* tissue. We chose to study merely the qualitative behaviour of ovules on mucosa because quantitative *ex vivo* protocols show high variability and poor reproducibility [77]. We observed that 3D printed ovules, administered as a solid

dosage form, soften to form an adhesive hydrogel on the mucosa. The mucoadhesive properties may facilitate retention, providing a longer contact time between the formulation and the mucosa and thus a longer period for vaginal drug absorption and a more controlled pharmacokinetic profile.

To estimate the required exposure time of pirfenidone, we chose 12Z, an immortalized human endometriotic cell line that recapitulates properties of endometriotic lesions including epithelial-to-mesenchymal transition, invasion and migration [62,63]. Pirfenidone acts by inhibiting TGF-β and thereby indirectly reducing cell proliferation [15,19]. Results from the metabolic assay suggest that low concentrations of pirfenidone (<1 mg/mL) for short exposure times (2–6 h) are insufficient to achieve a therapeutic effect, while high concentrations (>1 mg/mL) and long exposure times (24 h) are required for pirfenidone to act to reduce the metabolic activity of this endometriotic epithelial cell line. This highlights the need for a sustained release vaginal formulation that is able to achieve sustained high levels of pirfenidone locally.

We anticipate that our 3D printed dosage form, which shows advantageous *in vitro* release and *ex vivo* mucoadhesion properties, may enable pirfenidone levels to be sustained in the therapeutic window with better efficacy than Macrogol and Witepsol ovules.

Conclusion

In this work, we demonstrate that vaginal ovules manufactured using semisolid extrusion 3D printing using excipients generally recognised as safe are superior to standard moulded ovules in terms of *in vitro* release, and they have desirable *ex vivo* mucoadhesion properties. Despite the still relatively slow speed of manufacturing (about 40 min/ovule), the mucoadhesive and disintegration properties of the 3D printed ovules hold promise as vaginal drug delivery systems. Our assays suggest that pirfenidone may be absorbed through the vaginal mucosa and into systemic circulation. We expect good patient adherence using this dosage form, which incorporates a non-hormonal API, pirfenidone, and addresses fibrosis, a neglected aspect of endometriosis pathology. Future work will focus on performing *in vivo* studies to establish how much pirfenidone is absorbed vaginally and to pave the way for clinical trials.

Acknowledgements

We thank Milica Bulatovic and Thomas Hübscher for manufacturing the release test apparatus and agarose mould. Some images were created using BioRender.

Competing interests

The authors declare that they have no known competing financial interests or personal relationships that could have appeared to influence the work reported in this paper.

CRediT author statement

ST: conceptualization, methodology, investigation, formal analysis, writing – original draft, visualization; SA: methodology, formal analysis, visualization; JW: methodology, validation, investigation, visualization; MC – methodology; PL: conceptualization, writing – review & editing, supervision, project administration, funding acquisition.

References

[1] E.A. Stewart, C.L. Cookson, R.A. Gandolfo, R. Schulze-Rath, Epidemiology of uterine fibroids: a systematic review, BJOG An Int. J. Obstet. Gynaecol. 124 (2017) 1501–1512. https://doi.org/10.1111/1471-0528.14640.

[2] K.T. Zondervan, C.M. Becker, S.A. Missmer, Endometriosis, N. Engl. J. Med. 382 (2020) 1244–1256. https://doi.org/10.1056/NEJMra1810764.

[3] E.A. Stewart, S.K. Laughlin-Tommaso, W.H. Catherino, S. Lalitkumar, D. Gupta, B. Vollenhoven, Uterine fibroids, Nat. Rev. Dis. Prim. 2 (2016). https://doi.org/10.1038/nrdp.2016.43.

[4] P.T.K. Saunders, A.W. Horne, Endometriosis: Etiology, pathobiology, and therapeutic prospects, Cell. 184 (2021) 2807–2824. https://doi.org/10.1016/j.cell.2021.04.041.

[5] P. Viganò, J. Ottolina, L. Bartiromo, G. Bonavina, M. Schimberni, R. Villanacci, M. Candiani, Cellular Components Contributing to Fibrosis in Endometriosis: A Literature Review., J. Minim. Invasive Gynecol. 27 (2020) 287–295. https://doi.org/10.1016/j.jmig.2019.11.011.

[6] P. Viganò, M. Candiani, A. Monno, E. Giacomini, P. Vercellini, E. Somigliana, Time to redefine endometriosis including its pro-fibrotic nature, Hum. Reprod. 33 (2018) 347–352. https://doi.org/10.1093/humrep/dex354.

[7] C. Chapron, L. Marcellin, B. Borghese, P. Santulli, Rethinking mechanisms, diagnosis and management of endometriosis, Nat. Rev. Endocrinol. 15 (2019) 666–682.

https://doi.org/10.1038/s41574-019-0245-z.

[8] A.W. Horne, P.T.K. Saunders, SnapShot: Endometriosis, Cell. 179 (2019) 1677-1677.e1. https://doi.org/https://doi.org/10.1016/j.cell.2019.11.033.

[9] E.A. Stewart, R.A. Nowak, Uterine Fibroids: Hiding in Plain Sight, Physiology. 37 (2022) 16–27. https://doi.org/10.1152/physiol.00013.2021.

[10] S.W. Guo, Fibrogenesis resulting from cyclic bleeding: The Holy Grail of the natural history of ectopic endometrium, Hum. Reprod. 33 (2018) 353–356. https://doi.org/10.1093/humrep/dey015.

[11] M.S. Islam, A. Ciavattini, F. Petraglia, M. Castellucci, P. Ciarmela, Extracellular matrix in uterine leiomyoma pathogenesis: A potential target for future therapeutics, Hum. Reprod. Update. 24 (2018) 59–85. https://doi.org/10.1093/humupd/dmx032.

[12] J.M. Garcia Garcia, V. Vannuzzi, C. Donati, C. Bernacchioni, P. Bruni, F. Petraglia, Endometriosis: Cellular and Molecular Mechanisms Leading to Fibrosis, Reprod. Sci. (2022). https://doi.org/10.1007/s43032-022-01083-x.

[13] Esbriet 267 mg hard capsules summary of product characteristics, (2011). https://www.ema.europa.eu/en/medicines/human/EPAR/esbriet.

[14] Esbriet Prescribing Information, (2019). https://www.esbriethcp.com/dosing.html.

[15] R. Escutia-Gutiérrez, J.S. Rodríguez-Sanabria, C.A. Monraz-Méndez, J. García-Bañuelos, A. Santos-García, A. Sandoval-Rodríguez, J. Armendáriz-Borunda, Pirfenidone modifies hepatic miRNAs expression in a model of MAFLD/NASH, Sci. Rep. 11 (2021) 1–12. https://doi.org/10.1038/s41598-021-91187-2.

[16] G.J. Prud'homme, Pathobiology of transforming growth factor β in cancer, fibrosis and immunologic disease, and therapeutic considerations, Lab. Investig. 87 (2007) 1077–1091. https://doi.org/10.1038/labinvest.3700669.

[17] N.C. Henderson, F. Rieder, T.A. Wynn, Fibrosis: from mechanisms to medicines, Nature. 587 (2020) 555–566. https://doi.org/10.1038/s41586-020-2938-9.

[18] S.E. Bulun, Uterine Fibroids, N. Engl. J. Med. 369 (2013) 1344–1355. https://doi.org/10.1056/NEJMra1209993.

[19] S. Matsuzaki, J.-L. Pouly, M. Canis, Dose-dependent pro- or anti-fibrotic responses of endometriotic stromal cells to interleukin-1β and tumor necrosis factor α, Sci. Rep. 10 (2020) 9467. https://doi.org/10.1038/s41598-020-66298-x.

[20] B.S. Lee, S.B. Margolin, R.A. Nowak, Pirfenidone: A novel pharmacological agent that

inhibits leiomyoma cell proliferation and collagen production, J. Clin. Endocrinol. Metab. 83 (1998) 219–223. https://doi.org/10.1210/jcem.83.1.4503.

[21] P.S. Hasdemir, M. Ozkut, T. Guvenal, M.A. Uner, E. Calik, S.O. Koltan, F.M. Koyuncu, K. Ozbilgin, Effect of Pirfenidone on Vascular Proliferation, Inflammation and Fibrosis in an Abdominal Adhesion Rat Model, J. Investig. Surg. 30 (2017) 26–32. https://doi.org/10.1080/08941939.2016.1215578.

[22] A.S. El Halwagy, A.A. Al Gergawy, A.S. Dawood, A. Shehata, Reduction of Postoperative Adhesions after Laparoscopic Surgery for Endometriosis by Using a Novel Anti-Fibrotic Drug Pirfenidone: A Randomized Double Blind Study, Gynecol. Obstet. 07 (2017) 1–6. https://doi.org/10.4172/2161-0932.1000422.

[23] A. Hussain, F. Ahsan, The vagina as a route for systemic drug delivery, J. Control. Release. 103 (2005) 301–313. https://doi.org/https://doi.org/10.1016/j.jconrel.2004.11.034.

[24] C. Karavasili, G.K. Eleftheriadis, C. Gioumouxouzis, E.G. Andriotis, D.G. Fatouros, Mucosal drug delivery and 3D printing technologies: a focus on special patient populations, Adv. Drug Deliv. Rev. (2021) 113858. https://doi.org/10.1016/j.addr.2021.113858.

[25] L. Matteucci, A. Holmes, Vaginal epithelial drug delivery, Adv. Drug Deliv. Rev. (2022) 114293. https://doi.org/10.1016/j.addr.2022.114293.

[26] X. Wang, S. Liu, Y. Guan, J. Ding, C. Ma, Z. Xie, Vaginal drug delivery approaches for localized management of cervical cancer, Adv. Drug Deliv. Rev. 174 (2021) 114–126. https://doi.org/https://doi.org/10.1016/j.addr.2021.04.009.

[27] L.M. Ensign, R. Cone, J. Hanes, Nanoparticle-based drug delivery to the vagina: A review, J. Control. Release. 190 (2014) 500–514. https://doi.org/10.1016/j.jconrel.2014.04.033.

[28] N.J. Alexander, E. Baker, M. Kaptein, U. Karck, L. Miller, E. Zampaglione, Why consider vaginal drug administration?, Fertil. Steril. 82 (2004) 1–12. https://doi.org/https://doi.org/10.1016/j.fertnstert.2004.01.025.

[29] C. Bulletti, D. De Ziegler, C. Flamigni, E. Giacomucci, V. Polli, G. Bolelli, F. Franceschetti, Targeted drug delivery in gynaecology: The first uterine pass effect, Hum. Reprod. 12 (1997) 1073–1079. https://doi.org/10.1093/humrep/12.5.1073.

[30] E. Cicinelli, D. De Ziegler, Transvaginal progesterone: Evidence for a new functional “portal system” flowing from the vagina to the uterus, Hum. Reprod. Update. 5 (1999)

365–372. https://doi.org/10.1093/humupd/5.4.365.

[31] R.A. Miles, R.J. Paulson, R.A. Lobo, M.F. Press, L. Dahmoush, M. V Sauer, Pharmacokinetics and endometrial tissue levels of progesterone after administration by intramuscular and vaginal routes: a comparative study, Fertil. Steril. 62 (1994) 485–490. https://doi.org/https://doi.org/10.1016/S0015-0282(16)56935-0.

[32] S.K. Patel, G.R. Valicherla, A.C. Micklo, L.C. Rohan, Drug delivery strategies for management of women's health issues in the upper genital tract, Adv. Drug Deliv. Rev. 177 (2021) 113955. https://doi.org/10.1016/j.addr.2021.113955.

[33] E. Cicinelli, E. Di Naro, D. De Ziegler, M. Matteo, S. Morgese, P. Galantino, P.-A. Brioschi, S. Schonauer, Placement of the vaginal 17β-estradiol tablets in the inner or outer one third of the vagina affects the preferential delivery of 17β-estradiol toward the uterus or periurethral areas, thereby modifying efficacy and endometrial safety, Am. J. Obstet. Gynecol. 189 (2003) 55–58. https://doi.org/https://doi.org/10.1067/mob.2003.341.

[34] E. Cicinelli, D. de Ziegler, S. Morgese, C. Bulletti, D. Luisi, L.M. Schonauer, "First uterine pass effect" is observed when estradiol is placed in the upper but not lower third of the vagina, Fertil. Steril. 81 (2004) 1414–1416. https://doi.org/https://doi.org/10.1016/j.fertnstert.2003.12.016.

[35] D.R. Friend, Drug delivery for the treatment of endometriosis and uterine fibroids, Drug Deliv. Transl. Res. 7 (2017) 829–839. https://doi.org/10.1007/s13346-017-0423-2.

[36] T. Zaveri, R.J. Primrose, L. Surapaneni, G.R. Ziegler, J.E. Hayes, Firmness perception influences women's preferences for vaginal suppositories, Pharmaceutics. 6 (2014) 512–529. https://doi.org/10.3390/pharmaceutics6030512.

[37] A.J. Bakke, T. Zaveri, M.J. Higgins, G.R. Ziegler, J.E. Hayes, Design aspects of vaginal applicators that influence acceptance among target users, Sci. Rep. 11 (2021) 1–11. https://doi.org/10.1038/s41598-021-89284-3.

[38] S. Rençber, S.Y. Karavana, Z.A. Şenyiğit, B. Eraç, M.H. Limoncu, E. Baloğlu, Mucoadhesive in situ gel formulation for vaginal delivery of clotrimazole: formulation, preparation, and in vitro/in vivo evaluation, Pharm. Dev. Technol. 22 (2017) 551–561. https://doi.org/10.3109/10837450.2016.1163385.

[39] H. Ragelle, S. Rahimian, E.A. Guzzi, P.D. Westenskow, M.W. Tibbitt, G. Schwach, R. Langer, Additive manufacturing in drug delivery: innovative drug product design and opportunities for industrial application, Adv. Drug Deliv. Rev. (2021) 113990.

https://doi.org/10.1016/j.addr.2021.113990.

[40] J. Fu, X. Yu, Y. Jin, 3D printing of vaginal rings with personalized shapes for controlled release of progesterone, Int. J. Pharm. 539 (2018) 75–82. https://doi.org/https://doi.org/10.1016/j.ijpharm.2018.01.036.

[41] Z.-L. Farmer, E. Utomo, J. Domínguez-Robles, C. Mancinelli, E. Mathew, E. Larrañeta, D.A. Lamprou, 3D printed estradiol-eluting urogynecological mesh implants: Influence of material and mesh geometry on their mechanical properties, Int. J. Pharm. 593 (2021) 120145. https://doi.org/https://doi.org/10.1016/j.ijpharm.2020.120145.

[42] J. Domínguez-Robles, C. Mancinelli, E. Mancuso, I. García-Romero, B.F. Gilmore, L. Casettari, E. Larrañeta, D.A. Lamprou, 3D Printing of Drug-Loaded Thermoplastic Polyurethane Meshes: A Potential Material for Soft Tissue Reinforcement in Vaginal Surgery, Pharmaceutics. 12 (2020) 63. https://doi.org/10.3390/pharmaceutics12010063.

[43] K. Tappa, U. Jammalamadaka, D.H. Ballard, T. Bruno, M.R. Israel, H. Vemula, J.M. Meacham, D.K. Mills, P.K. Woodard, J.A. Weisman, Medication eluting devices for the field of OBGYN (MEDOBGYN): 3D printed biodegradable hormone eluting constructs, a proof of concept study, PLoS One. 12 (2017) e0182929. https://doi.org/10.1371/journal.pone.0182929.

[44] T. Tagami, N. Hayashi, N. Sakai, T. Ozeki, 3D printing of unique water-soluble polymer-based suppository shell for controlled drug release, Int. J. Pharm. 568 (2019) 118494. https://doi.org/https://doi.org/10.1016/j.ijpharm.2019.118494.

[45] K. Paul, S. Darzi, G. McPhee, M.P. Del Borgo, J.A. Werkmeister, C.E. Gargett, S. Mukherjee, 3D bioprinted endometrial stem cells on melt electrospun poly ε-caprolactone mesh for pelvic floor application promote anti-inflammatory responses in mice, Acta Biomater. 97 (2019) 162–176. https://doi.org/https://doi.org/10.1016/j.actbio.2019.08.003.

[46] Ph. Eur. 10.8 1164 (01/2008), (n.d.). https://www.edqm.eu/en/european-pharmacopoeia-ph-eur-10th-edition-.

[47] V. Kale, R. Trivedi, P. Muley, Proposed design of a dissolution apparatus for vaginal formulations containing probiotics, Dissolution Technol. 15 (2008) 27–29. https://doi.org/10.14227/DT150208P27.

[48] E. Baloglu, Z. Ay Senyigit, S.Y. Karavana, A. Vetter, D.Y. Metin, S. Hilmioglu Polat, T. Guneri, A. Bernkop-Schnurch, In vitro evaluation of mucoadhesive vaginal tablets of

antifungal drugs prepared with thiolated polymer and development of a new dissolution technique for vaginal formulations, Chem. Pharm. Bull. 59 (2011) 952–958. https://doi.org/10.1248/cpb.59.952.

[49] J. Gupta, J.Q. Tao, S. Garg, R. Al-Kassas, Design and Development of an in Vitro Assay for Evaluation of Solid Vaginal Dosage Forms, Pharmacol. Pharm. 02 (2011) 289–298. https://doi.org/10.4236/pp.2011.24037.

[50] M. Falavigna, M. Pattacini, R. Wibel, F. Sonvico, N. Škalko-Basnet, G.E. Flaten, The vaginal-PVPA: A vaginal mucosa-mimicking in vitro permeation tool for evaluation of mucoadhesive formulations, Pharmaceutics. 12 (2020) 1–15. https://doi.org/10.3390/pharmaceutics12060568.

[51] S. Klein, K. Tietz, Vaginal and Intrauterine Delivery Systems Vaginal and Uterine Anatomy and Physiology Relevant to Drug Delivery, in: Vitr. Drug Release Test. Spec. Dos. Forms, John Wiley & Sons, Ltd, 2020: pp. 177–209.

[52] K. Tietz, Entwicklung diskriminierender und bioprädiktiver Methoden zur Bestimmung der Wirkstofffreisetzung aus langwirksamen kontrazeptiven Darreichungsformen, Universität Greifswald, 2019.

[53] R.L. Shapiro, K. DeLong, F. Zulfiqar, D. Carter, M. Better, L.M. Ensign, In vitro and ex vivo models for evaluating vaginal drug delivery systems, Adv. Drug Deliv. Rev. 191 (2022) 114543. https://doi.org/10.1016/J.ADDR.2022.114543.

[54] D.H. Owen, D.F. Katz, A vaginal fluid simulant, Contraception. 59 (1999) 91–95. https://doi.org/10.1016/S0010-7824(99)00010-4.

[55] R. Rastogi, J. Su, A. Mahalingam, J. Clark, S. Sung, T. Hope, P.F. Kiser, Engineering and characterization of simplified vaginal and seminal fluid simulants, Contraception. 93 (2016) 337–346. https://doi.org/10.1016/j.contraception.2015.11.008.

[56] Vaginal preparations - European Pharmacopoeia 11.1, (n.d.). https://pheur.edqm.eu/app/11-1/content/11-1/1164E.htm?highlight=on&terms=vaginalia (accessed October 12, 2022).

[57] C.A. Santos, J.S. Jacob, B.A. Hertzog, B.D. Freedman, D.L. Press, P. Harnpicharnchai, E. Mathiowitz, Correlation of two bioadhesion assays: the everted sac technique and the CAHN microbalance, J. Control. Release. 61 (1999) 113–122. https://doi.org/https://doi.org/10.1016/S0168-3659(99)00109-1.

[58] J. Bassi da Silva, S.B. de S. Ferreira, O. de Freitas, M.L. Bruschi, A critical review about methodologies for the analysis of mucoadhesive properties of drug delivery

systems, Drug Dev. Ind. Pharm. 43 (2017) 1053–1070. https://doi.org/10.1080/03639045.2017.1294600.

[59] A. Zeitvogel, R. Baumann, A. Starzinski-Powitz, Identification of an invasive, N-cadherin-expressing epithelial cell type in endometriosis using a new cell culture model, Am. J. Pathol. 159 (2001) 1839–1852. https://doi.org/10.1016/S0002-9440(10)63030-1.

[60] G. Valentino, C. Zivko, F. Weber, L. Brülisauer, P. Luciani, Synergy of phospholipid—drug formulations significantly deactivates profibrogenic human hepatic stellate cells, Pharmaceutics. 11 (2019) 676. https://doi.org/10.3390/pharmaceutics11120676.

[61] R. Palmeira-de-Oliveira, A.S. Oliveira, J. Rolo, M. Tomás, A. Palmeira-de-Oliveira, S. Simões, J. Martinez-de-Oliveira, Women's preferences and acceptance for different drug delivery routes and products, Adv. Drug Deliv. Rev. 182 (2022) 114133. https://doi.org/10.1016/j.addr.2022.114133.

[62] A. Stejskalová, V. Fincke, M. Nowak, Y. Schmidt, K. Borrmann, M.K. von Wahlde, S.D. Schäfer, L. Kiesel, B. Greve, M. Götte, Collagen I triggers directional migration, invasion and matrix remodeling of stroma cells in a 3D spheroid model of endometriosis, Sci. Rep. 11 (2021) 1–15. https://doi.org/10.1038/s41598-021-83645-8.

[63] J.J. Reske, M.R. Wilson, B. Armistead, S. Harkins, C. Perez, J. Hrit, M. Adams, S.B. Rothbart, S.A. Missmer, A.T. Fazleabas, R.L. Chandler, ARID1A-dependent maintenance of H3.3 is required for repressive CHD4-ZMYND8 chromatin interactions at super-enhancers, BMC Biol. 2022 201. 20 (2022) 1–26. https://doi.org/10.1186/S12915-022-01407-Y.

[64] B.D. McKinnon, S.W. Lukowski, S. Mortlock, J. Crawford, S. Atluri, S. Subramaniam, R.L. Johnston, K. Nirgianakis, K. Tanaka, A. Amoako, M.D. Mueller, G.W. Montgomery, Altered differentiation of endometrial mesenchymal stromal fibroblasts is associated with endometriosis susceptibility, Commun. Biol. 2022 51. 5 (2022) 1–14. https://doi.org/10.1038/s42003-022-03541-3.

[65] Y. Mohammed, A. Holmes, P.C.L. Kwok, T. Kumeria, S. Namjoshi, M. Imran, L. Matteucci, M. Ali, W. Tai, H.A.E. Benson, M.S. Roberts, Advances and future perspectives in epithelial drug delivery, Adv. Drug Deliv. Rev. 186 (2022) 114293. https://doi.org/10.1016/j.addr.2022.114293.

[66] R. Palmeira-De-Oliveira, P. Duarte, A. Palmeira-De-Oliveira, J. Das Neves, M.H. Amaral, L. Breitenfeld, J. Martinez-De-Oliveira, Women's experiences, preferences and perceptions regarding vaginal products: Results from a cross-sectional web-based

survey in Portugal, Https://Doi.Org/10.3109/13625187.2014.980501. 20 (2015) 259–271. https://doi.org/10.3109/13625187.2014.980501.

[67] L.K. Shum, M.A. Bedaiwy, C. Allaire, C. Williams, H. Noga, A. Albert, S. Lisonkova, P.J. Yong, Deep Dyspareunia and Sexual Quality of Life in Women With Endometriosis, Sex. Med. 6 (2018) 224–233. https://doi.org/10.1016/J.ESXM.2018.04.006.

[68] V.F. Cervi, C.P. Saccol, T. da Rosa Pinheiro, R.C.V. Santos, M.H.M. Sari, L. Cruz, A novel nanotechnological mucoadhesive and fast-dissolving film for vaginal delivery of clotrimazole: design, characterization, and in vitro antifungal action, Drug Deliv. Transl. Res. (2022) 1–13. https://doi.org/10.1007/S13346-022-01154-1/FIGURES/6.

[69] B. Shrestha, K. Vincent, A. Schaefer, Y. Zhu, G. Vargas, M. Motamedi, K. Swope, J. Morton, C. Simpson, H. Pham, M.B. Brennan, M.H. Pauly, L. Zeitlin, B. Bratcher, K.J. Whaley, T.R. Moench, S.K. Lai, Hexavalent sperm-binding IgG antibody released from vaginal film for development of potent on-demand nonhormonal female contraception, Proc. Natl. Acad. Sci. U. S. A. 118 (2021) e2107832118. https://doi.org/10.1073/PNAS.2107832118/SUPPL_FILE/PNAS.2107832118.SD01.XLSX.

[70] J.A. Politch, S. Cu-Uvin, T.R. Moench, K.T. Tashima, J.G. Marathe, K.M. Guthrie, H. Cabral, T. Nyhuis, M. Brennan, L. Zeitlin, H.M.L. Spiegel, K.H. Mayer, K.J. Whaley, D.J. Anderson, Safety, acceptability, and pharmacokinetics of a monoclonal antibody-based vaginal multipurpose prevention film (MB66): A Phase I randomized trial, PLOS Med. 18 (2021) e1003495. https://doi.org/10.1371/JOURNAL.PMED.1003495.

[71] Safety and Pharmacokinetics of Two Vaginal Film Formulations Containing the Integrase Inhibitor MK-2048 - Full Text View - ClinicalTrials.gov, (n.d.). https://clinicaltrials.gov/ct2/show/NCT04319718 (accessed October 12, 2022).

[72] A. Dedeloudi, A. Siamidi, P. Pavlou, M. Vlachou, Recent Advances in the Excipients Used in Modified Release Vaginal Formulations, Materials (Basel). 15 (2022). https://doi.org/10.3390/ma15010327.

[73] S. Adepu, S. Ramakrishna, R. Costa-Pinto, A.L. Oliveira, Controlled Drug Delivery Systems: Current Status and Future Directions, Molecules. 26 (2021) 5905. https://doi.org/10.3390/MOLECULES26195905.

[74] 5.17.1. Recommendations on dis... - European Pharmacopoeia 11.1, (n.d.). https://pheur.edqm.eu/app/11-1/content/11-1/51701E.htm?highlight=on&terms=5.17.1 (accessed October 13, 2022).

[75] USP-NF ⟨711⟩ Dissolution, (n.d.). https://online.uspnf.com/uspnf/document/1_GUID-AC788D41-90A2-4F36-A6E7-769954A9ED09_2_en-US#C711S11 (accessed October 13, 2022).

[76] C. Bassand, J. Verin, M. Lamatsch, F. Siepmann, J. Siepmann, How agarose gels surrounding PLGA implants limit swelling and slow down drug release, J. Control. Release. 343 (2022) 255–266. https://doi.org/10.1016/J.JCONREL.2022.01.028.

[77] M.N. Pereira, T.A. Reis, B.N. Matos, M. Cunha-Filho, T. Gratieri, G.M. Gelfuso, Novel ex vivo protocol using porcine vagina to assess drug permeation from mucoadhesive and colloidal pharmaceutical systems, Colloids Surfaces B Biointerfaces. 158 (2017) 222–228. https://doi.org/10.1016/j.colsurfb.2017.07.008.

[78] C.C. Davis, M. Baccam, M.J. Mantz, T.W. Osborn, D.R. Hill, C.A. Squier, Use of porcine vaginal tissue ex-vivo to model environmental effects on vaginal mucosa to toxic shock syndrome toxin-1, Toxicol. Appl. Pharmacol. 274 (2014) 240–248. https://doi.org/10.1016/j.taap.2013.11.021.

[79] C.A. Squier, M.J. Mantz, P.M. Schlievert, C.C. Davis, Porcine vagina ex vivo as a model for studying permeability and pathogenesis in mucosa, J. Pharm. Sci. 97 (2008) 9–21. https://doi.org/10.1002/jps.21077.

[80] A.D. Van Eyk, P. Van Der Bijl, Porcine vaginal mucosa as an in vitro permeability model for human vaginal mucosa, Int. J. Pharm. 305 (2005) 105–111. https://doi.org/10.1016/J.IJPHARM.2005.09.002.

CRediT author statement

ST: conceptualization, methodology, investigation, formal analysis, writing – original draft, visualization;

SA: methodology, formal analysis, visualization;

JW: methodology, validation, investigation, visualization;

MC – methodology;

PL: conceptualization, writing – review & editing, supervision, project administration, funding acquisition.

GA